Structural, optical and antibacterial properties of yttrium doped ZnO nanoparticles

(Propriedades estruturais, ópticas e antibacterianas de nanopartículas de ZnO dopadas com ítrio)

V. D. Mote[1*], Y. Purushotham[2], R. S. Shinde[3], S. D. Salunke[3], B. N. Dole[4]
[1]Department of Physics, Dayanand Science College, Latur - 413 512, India
[2]Centre for Materials for Electronics Technology, Cherlapally, Hyderabad - 500 051, India
[3]Department of Chemistry, RajarshiShahuMahavidyalay, Latur - 413 512, India
[4]Advanced Materials Research Laboratory, Department of Physics, Dr. B. A. M. University, Aurangabad - 431 004, India
**corresponding author: motevd15@gmail.com*

Abstract

Yttrium-doped ZnO nanoparticles were synthesized by co-precipitation method to investigate structural, optical and antibacterial properties. X-ray diffraction analysis confirms hexagonal (wurtzite) structure with average crystallite size between 16 and 30 nm. Optical energy band gap decreaseswith increasing Y-doping concentration. ZnO nanoparticles were found to be highly effective against *S. aureus* and Y-doped ZnO nanoparticles against *E. coli, B. subtilis* and *S. typhi*. Undoped and Y-doped ZnO nanoparticles are good inorganic antimicrobial agents and can be synthesized by cost effective co-precipitation method.
Keywords: nanoparticles, ZnO, coprecipitation, antibacterial properties.

Resumo

Nanopartículas de ZnO dopado com ítrio foram sintetizadas pelo método de coprecipitação para investigar as propriedades estruturais, ópticas e antibacterianas. A análise de difração de raios X confirma a estrutura hexagonal (wurtzita) com tamanho médio de cristalito entre 16 e 30 nm. O gap de energia óptica diminui com o aumento da concentração do dopante Y. Foi verificado qu nanopartículas de ZnO sãoaltamente eficazes para S. aureus e nanopartículas de ZnO dopado com Y para E. coli, B. subtilis e S. typhi. Nanopartículas de ZnO não dopad*as e dopadas com Y* são bons agentes antimicrobianos inorgânicos e pode*m ser sintetizadas pelo método de baixo custo de coprecipitação.*
***Palavras-chave**: nanopartículas, ZnO, coprecipitação, propriedades antibacterianas.*

INTRODUCTION

Semiconductor nanoparticles have attracted much attention in the industrial and energy production applications [1-3]. ZnO nanoparticles exhibit excellent electrical, opticaland chemical properties, widely applied to produce semiconductors, optical devices, piezoelectric devices, surface acoustic wave devices, sensors, transparent electrodes and solar cells [4-6]. Besides, ZnO nanoparticles also exhibiting antimicrobial activities against *Escherichiacoli* and *Staphylococcus aureus* [7-11]. Several researchers reported doping of ZnO with metals such as Mn, Co, Cr, Cu, In and Laby various methods such as hydrothermal, sol-gel and coprecipitation method but only few reports are available ZnO doped with Al and Y [12-16].

In view of the above, pure and Y-doped ZnO nanoparticles synthesized by cost effective co-precipitation method and characterized by XRD, TEM, UV-Vis and bacterial activities were investigated. Results are presented in this paper.

EXPERIMENTAL

Samples with compositional formula $Zn_{1-x}Y_xO$, with x = 0.00, 0.05, 0.10 and 0.15 were prepared by co-precipitation route in an alcoholic medium. In this procedure, zinc acetate dehydrate dissolved in methanol (100 mL) and NaOH in methanol (100 mL) were prepared and added by stirring with heating at 52 °C for 2 h. The precipitate separated from the solution by filtration, washed several times with distilled water and ethanol then dried in air at 127 °C to obtain ZnO nanoparticles. The samples obtained were annealed at 450 °C for 8 h. For the synthesis of Y-doped ZnO nanoparticles, zinc acetate dehydrate and yttrium acetate tetrahydrate were dissolved in methanol (100 mL) and NaOH in methanol (100 mL) were prepared and added by stirring with heating at 52 °C for 2 h. The precipitate separated from the solution by filtration, washed several times with distilled water and ethanol then dried in air at 127 °C to obtain Y-doped ZnO nanoparticles. The samples were annealed at 450 °C for 8 h.

The crystalline structure, phase purity and size of the nanoparticles were determined by XRD (Philips PW-3710). Optical properties of the samples were recorded using UV-Vis spectrophotometer (Jasco) in the range 200-800 nm.

Anti-bacterial studies: nutrient broth (1.3 g) dissolved in 100 mL distilled water, pH adjusted to 6.8 then sterilized in autoclave at 121 °C for 20 min (15 lb). Nutrient agar (2.5 g) added tothe distilled water by adjusting pH then autoclaved at 121 °C for 20 min (15 lb). Pure cultures of bacteria *E. coli, B. subtilis, S. typhi* and *S. aureus* were used.

Preparation of Inolculum:100 mL nutrient broth distributed 25 mL each in 4 conical flasks labeled as *E. coli, B. subtilis, S. typhi* and *S. aureus* and autoclaved at 121 °C for 20 min. Pure culture of all these clinically isolated strain bacteria were added to each conical flask, kept on rotary shaker for 24 h at 37 °C.

Preparation and Inoculation of test plates: Nutrient broth (1.3 g) and Agar (2.5 g) mixed in 100 mL distilled water and sterilized in autoclave at 121 °C for 20 min then poured into sterile petriplates (15-20 mL) to solidify. Plates were labeled for each test organism then pure cultures of test organisms spreaded entire surface of the plates by swabbing in three directions. Plates were allowed to dry for 5 min. Then wells were cut on each plate with sterile cup borer and labeled as S1, S2, S3, S4. Each sample was then loaded with sterile pipettes in respective plates. Plates were incubated at 37 °C for 24 h.

RESULTS AND DISCUSSION

Structural properties

XRD patterns of undoped and Y-doped ZnO nanoparticles are shown in Fig. 1, all samples showing hexagonal ZnO phase and indexed peaks correspond to (100), (002), (101)

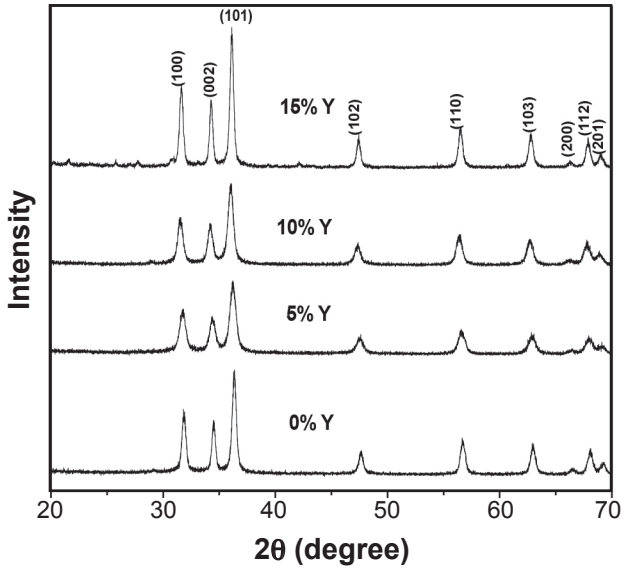

Figure 1: XRD patterns of pure and Y-doped ZnO nanoparticles.
[Figura 1: Difratogramas de raios X de nanopartículas de ZnO puro e dopado com Y.]

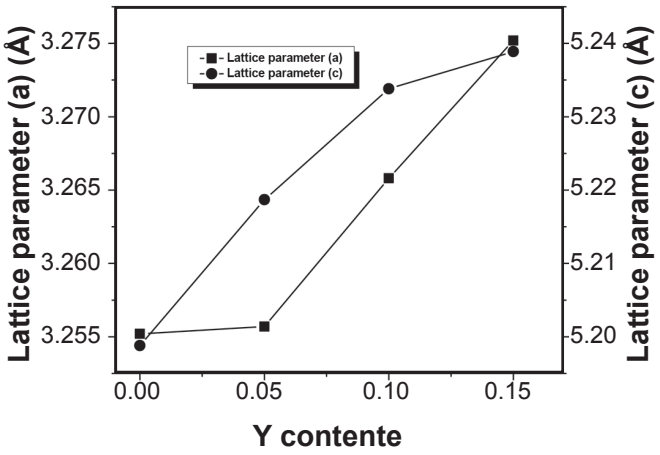

Figure 2: Variation of lattice parameter (a and c)with Y content of $Zn_{1-x}Y_xO$ nanoparticles.
[Figura 2: Variação do parâmetro de rede (a e c) com teor de Y de nanopartículas de $Zn_{1-x}Y_xO$.]

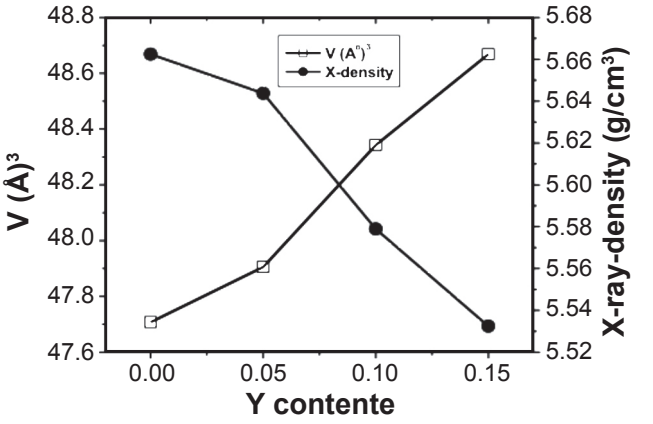

Figure 3: Unit cell volume and X-ray density vs Y concentration.
[Figura 3: Volume da célula unitária e densidade por difração de raios X em função da concentração de Y.]

and (110) are matching well with the JCPDS data. Further, there are no extra impurities or formations of any phase of Y were detected in the prepared samples. Yttrium doping shows a pronounced effect on the lattice parameters of 'a' and 'c' as compared to undoped ZnO. The lattice parameters increased with increasing Y concentration as shown in Fig. 2. Similar trend for was reported for Y-doped ZnS nanoparticles [17]. The unit cell volume is also following similar trend. This is attributed to ionic radius difference between Zn (0.74 Å) and Y (1.04 Å) ions. The variation of unit cell volume and X-ray density with Y content is shown in Fig 3. X-ray density decreases with increasing Y concentration, indicating the substitution of Y ions in ZnO nanoparticles. All values are in Table I.

Bond lengthof doped and undoped ZnO are shown in Table II. It is found that the bond length values of perpendicular ($C\perp$) as well as parallel ($C_{||}$) to c-axis increasing with increasing Y concentration. It could be due to the induced growth of the particle at higher temperature.

Table I - Lattice parameters, unit cell volume and X-ray density of Y-doped ZnO nanoparticles.
[Tabela I - Parâmetros de rede, volume da célula unitária e densidade obtida por difração de raios X de nanopartículas de ZnO dopado com Y.]

Sample code	Y concentration (x)	a (Å)	c (Å)	V (Å^3)	X-ray density (g/cm^3)
S1	0.00	3.2552	5.1988	47.7078	5.6624
S2	0.05	3.2557	5.2187	47.9051	5.6437
S3	0.10	3.2658	5.2338	48.3423	5.5789
S4	0.15	3.2752	5.2389	48.6683	5.5324

The lattice distortion (ε_v) was calculated using following equation:

$$\varepsilon_v = \frac{a^2c - a_0^2c_0}{a_0^2c_0} \quad (A)$$

where a_0 and c_0 are the lattice parameters of pure ZnO single crystal. The ε_v values are shown in Table II and are enhancing with increasing Y. It indicates that Y ions go into Zn crystallographic 2b site in ZnO crystal structure. Further, the atomic packing fraction (APF) was also calculated using XRD data and found that APF in the range of 75-76%. The crystalline size correspond to the most pronounce diffraction peak (101) has been calculated using Debye-Scherrer's formula

$$D = \frac{K\lambda}{\beta_{hkl}\,Cos\theta} \quad (B)$$

where K is the shape factor, λ is wavelength, β_{hkl} is the full width at half maximum, θ is glancing angle. Table II summaries the results of crystallite sizes. The average crystalline size is in the range of 16-30 nm.

Optical properties

The UV-Vis absorption spectra of pure and Y doped nanoparticles are shown in Fig. 4 and vary linearly with increasing Y concentration. This may be due to the change in the average crystallite size of nanoparticles. Using optical absorption data, band gap energies were calculated.

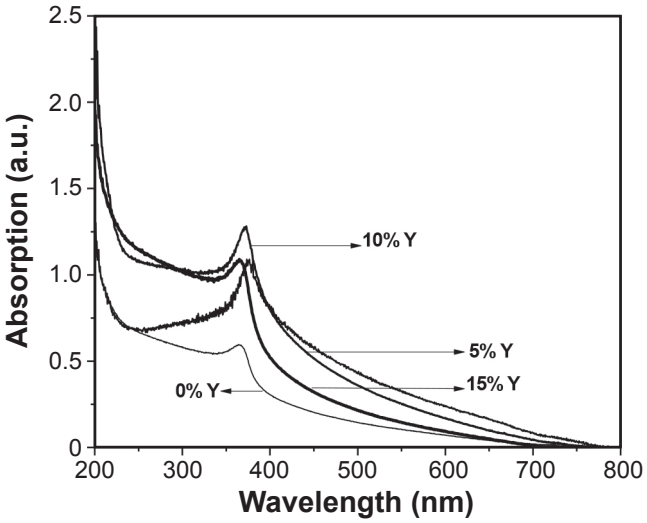

Figure 4: UV-Vis spectra of Y-doped ZnO nanoparticles.
[Figura 4: Espectros UV-Vis de nanopartículas de ZnO dopado com Y.]

As per theory of inter band optical absorption, at the absorption edge, the optical absorption coefficient ($\alpha h\nu$) varies with the photon energy ($h\nu$) according to the following expression

$$(\alpha h\nu)^n = A(h\nu - E_g) \quad (C)$$

Table II - Bond length, lattice distortion parameter, crystallite size and APF of ZnO nanoparticles.
[Tabela II - Comprimento de ligação, parâmetro distorção da rede, tamanho de cristalito e APF de nanopartículas de ZnO.]

Samples	C⊥	C$_{\|\|}$	ε_v	D (nm)	APF
S1	1.9933	1.9746	0.001751	26.1157	0.75675
S2	1.9937	1.9779	0.005905	16.9898	0.75398
S3	1.9998	1.9839	0.015058	19.4205	0.75414
S4	2.0056	1.9880	0.021605	29.5443	0.75557

where A is constant, E_g band gap energy and n is a number which characterizes the transition process.

The absorption coefficient (α) is calculated using the equation

$$a = 2.303\left(\frac{A}{t}\right) \quad (D)$$

where A is the absorption and t is the thickness of cuvate, i.e., 1 cm. The E_g values for direct and indirect transition obtained by the plots of $(\alpha h\nu)^2$ Vs photon energy ($h\nu$) and are shown in Fig 5. The optical band gap energies are found to be 3.16, 2.99, 2.68, 2.66 eV and are decreasing with increasing Y concentration. The values are relatively smaller than that of bulk ZnO (3.34 eV). This maybe due to average crystallite size and quantum confinement effect on Y doped ZnO nanoparticles.

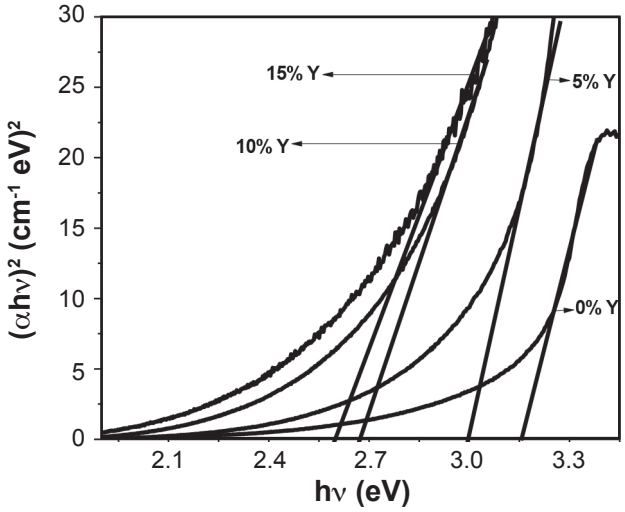

Figure 5: Photon energy $(\alpha h\nu)^2$ against ($h\nu$) of the Y-doped ZnO nanoparticles.
[Figura 5: Energia dos fótons $(\alpha h\nu)^2$ em função de (hν) das nanopartículas de ZnO dopado com Y.]

Antibacterial activity

Well diffusion method is used for the assessment of antibacterial activity and the results are shown in Figs. 6-9. S_2 and S_3 samples are not showing any antibacterial activity against any of the test microorganisms, whereas, S_1 showingmaximum antibacterial activity against *S.aureus* and S_4 sample showing maximum antibacterial activity against *B.subtilis* (18 mm), followed by *E. coli* and *S. typhi* (16 mm both) and no antibacterial activity against *S.aureus*. Undoped ZnO nanoparticles (S_1) showing maximum antibacterial activity against *S. aureus*, i.e., 18 nm as compared to 15% Y doped (S_4) ZnO nanoparticles (16 mm). Other microorganisms *E. coli, S. typhi* and *B. subtils* was not detected the antibacterial activity. Several researchers reported the antibacterial activity of undoped ZnO for *E.coli* [18, 19]. Zone of inhibition observed against pathogenic bacteria suggests that ZnO nanoparticles exhibit excellent

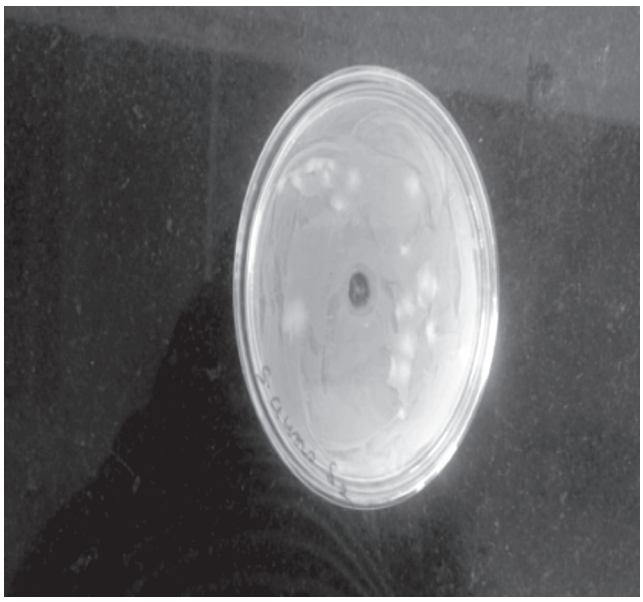

Figure 6: S_1 sample activity against *S. aureus.*
[Figura 6: Atividade da amostra S_1 para S. aureus.]

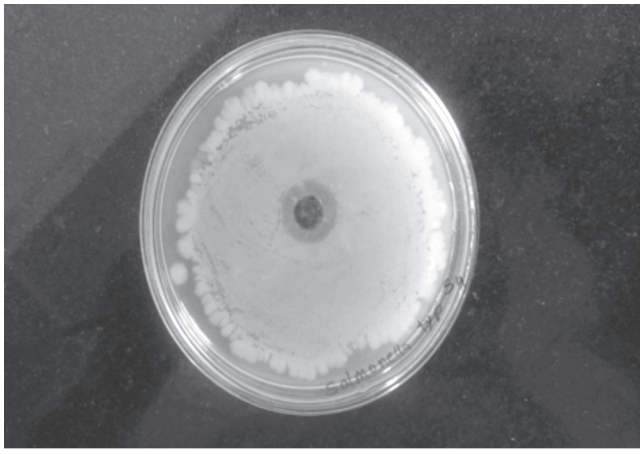

Figure 7: S_4 sample activity against *S. typhi.*
[Figura 7: Atividade da amostra S_4 para S. typhi.]

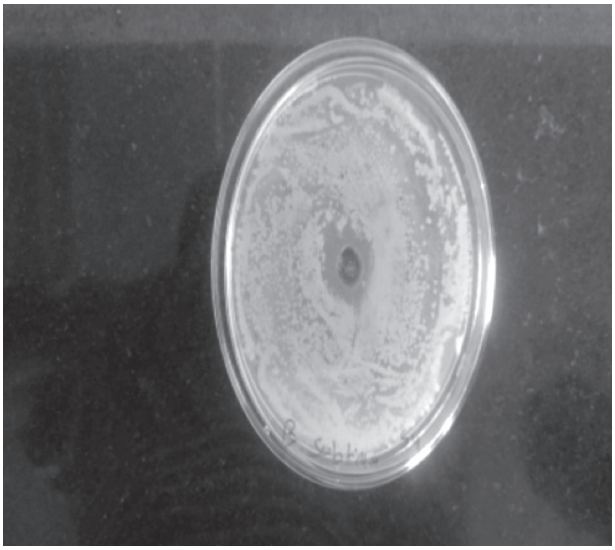

Figure 8: Activity of S_4 sample against *B. subtilis.*
[Figura 8: Atividade da amostra S_4 para B. subtilis.]

Figure 9: Activity of S_4 sample against *E. coli.*
[Figura 9: Atividade da amostra S_4 para E. coli.]

antibacterial activity for *S. aureus*.The antibacterial activity of ZnO nanoparticles depends on its size, surface area and concentration. The inhibitory effect increases with increasing Y concentration. The antibacterial activity results of pure ZnO and Y doped ZnO nanoparticles are in good agreement with reported literature [20-22].

CONCLUSIONS

Pure and yttrium-doped ZnO nanoparticles were synthesized by the co-precipitation method. Lattice parameters and unit cell volume increases with increasing Y concentration, indicating successful doping of Y ions into ZnO lattice. The average crystalline size is in the range 16-30 nm. The energy band gap decreases with increasing Y content. Antibacterial activity was observed using the disc diffusion method. Undoped ZnO (S_1) nanoparticles have antibacterial activity against *S. aureus*. The doping of Y in ZnO (S_4) increases its potential against *E. coli, B. subtilis, S. typhi* and no effect against *S. aureus*.

REFERENCES

[1] A. Erdem, Talanta **74** (2007) 318.
[2] G.Q. Wang, Y.Q. Wang, L.X. Chen, J. Choo, Biosens. Bioelectron. **25** (2010) 1859.
[3] A.M. O'Mahony, J. Wang, Anal. Methods **5** (2013) 4296.
[4] W. Park, G.C. Yi, J.W. Kim, S.M. Park, Appl. Phys. Lett. **82** (2003) 4358.
[5] Z. Liu, Z. Jin, W. Li, J. Qiu, Mater. Lett. **59** (2005) 3620.
[6] A. Moezzi, A.M. McDonagh, M.B. Cortie, Chem. Eng. J. **1**(2012) 185.
[7] K. Tam, A. Djurišić, C. Chan, Y. Xi, C. Tse, Y. Leung, W. Chan, F. Leung, D. Au, Thin Solid Films **516** (2008) 6167.
[8] O. Yamamoto, M. Komatsu, J. Sawai, Z. Nakagawa, J. Mater. Sci.- Mater. Med. **15** (2004) 847.
[9] V. Ischenko, S. Polarz, D. Grote, V. Stavarache, K. Fink, M. Driess, Adv. Funct. Mater. **15** (2005) 1945.
[10] L. Znaidi, G.J.A.A. SolerIllia, S. Benyahia, C. Sanchez, A.V.Kanaev, Thin Solid Films **428** (2003) 257.
[11] C. Wu, X. Qiao, J. Chen, H. Wang, Mater. Chem. Phys. **102** (2007) 7.
[12] A. Kargar, Y. Jing, S.J. Kim, C.T. Riley, X. Q. Pan, D.L. Wang, ACS Nano **7** (2013)11112.
[13] S. Martha, K.H. Reddy, K.M. Parida, J. Mater. Chem. A **2** (2014) 3621.
[14] T. Surendar, S. Kumar, V. Shanker, Phys. Chem. Chem.Phys.**16** (2014) 728.
[15] J.-D. Wang, J.-K. Liu, Q. Tong, Y. Lu, X.-H. Yang, Ind. Eng. Chem. Res. **53** (2014) 2229.
[16] P.K. Sanoop, S. Anas, S. Ananthakumar, V. Gunasekar, R. Saravanan, V. Ponnusami, Arab. J. Chem., DOI: 10.1016/j.arabjc.2012.04.023, **54** (2012).
[17] R. Viswanath, H.S.B. Naik, Y.K.G. Somalanaik, P.K.P. Neelanjeneallu, K.N. Harish, M.C. Prabhakara, J. Nanotech., article ID 924797, 8 pages (2014).
[18] J.P. Huo, J.C. Luo, W. Wu, J.F. Xiong, G.Z. Mo, Y. Wang, Ind. Eng. Chem. Res. **52** (2013) 11850.
[19] A. Stoyanova, H. Hitkova, A. Bachvarova-Nedelcheva, R. Iordanova, N. Ivanova, M. Sredkova, J. Chem. Tech. Metall. **48** (2013) 154.
[20] M.A. Gondal, A.J. Alzahrani, M.A. Randhawa, M.N. J. Siddiqui, Env. Sci. Health Part A **47** (2012) 1413.
[21] O. Yamamoto, M. Komatsu, J. Sawai, Z.E. Nakagawa, J. Mater. Sci. **15** (2004) 847.
[22] H. Lie, Chin. Sci. Bull. **6** (2014) 514.
(Rec. 21/05/2015, Ac. 30/07/2015)